Frontiers in Bioscience Landmark

Front. Biosci. (Landmark Ed) **2023**; 28(9): 205
https://doi.org/10.31083/j.fbl2809205

Original Research

Zbtb14 Promotes Non-Alcoholic Fatty Liver Disease-Associated Fibrosis in Gerbils via the β-Catenin Pathway

Guocan Chen[1], Xiaobing Wang[2], Yongfen Zhu[3], Huiying Hu[4], Xiaofeng Chu[4,*]

[1]Center for Drug Safety Evaluation, Hangzhou Medical College, 310013 Hangzhou, Zhejiang, China
[2]Medical School of Jinhua Polytechnic, 321016 Jinhua, Zhejiang, China
[3]Department of Hepatology and Infection, Sir Run Run Shaw Hospital, Affiliated with School of Medicine, Zhejiang University, 310020 Hangzhou, Zhejiang, China
[4]High Level Bio-safety Laboratory, Hangzhou Medical College, 310013 Hangzhou, Zhejiang, China
*Correspondence: cxf1001@hmc.edu.cn (Xiaofeng Chu)
Academic Editor: Nadia Diano
Submitted: 26 November 2022 Revised: 16 March 2023 Accepted: 23 March 2023 Published: 15 September 2023

Abstract

Background: Non-alcoholic fatty liver disease (NAFLD) is a popular chronic liver disorder with high morbidity and with no approved therapeutic drugs. Fibrosis is a crucial drug efficacy indicator for NAFLD. Thus, investigating the mechanisms of NAFLD-associated fibrosis and exploring effective therapeutic targets is imperative. **Methods**: Gerbil NAFLD-associated fibrosis model was constructed by feeding a high-fat and high-cholesterol diet. The hematoxylin and eosin staining and the alanine transaminase (ALT) and aspartate transaminase (AST) assays were used to determine liver tissue injury. Masson staining and hydroxyproline (Hyp) level determination were used to assess liver fibrosis. High-throughput mRNA sequencing was used to screen differentially expressed genes in the NAFLD-associated fibrosis model. Cell Counting Kit-8 was utilized to test cell viability. **Results**: Liver injury and fibrosis were observed in the gerbil NAFLD-associated fibrosis model with increased ALT, AST, and Hyp levels. The screened differentially expressed genes were mainly enriched in "negative regulation of hemopoiesis", "response to interleukin-1", and "granulocyte migration". Zinc Finger and BTB Domain Containing 14 (Zbtb14) was upregulated in liver tissues of the gerbil NAFLD-associated fibrosis model, patients with liver fibrosis, and hepatic stellate cells (HSCs). Additionally, Zbtb14 regulated primary HSCs activation via the β-catenin pathway. **Conclusions**: Zbtb14 regulated NAFLD-associated fibrosis via the β-catenin pathway, for the first time, and it serves as the probable target for NAFLD therapy.

Keywords: non-alcoholic fatty liver disease; fibrosis; hepatic stellate cells; Zbtb14; β-catenin

1. Introduction

Non-alcoholic fatty liver disease (NAFLD) is a chronic liver disorder with global prevalence [1]. Globally, 25% adults and 90% obese populations suffer from NAFLD [1–3]. Therefore, NAFLD is a huge threat to public health. NAFLD is a metabolic disease that presents as lipid deposition in liver cells but without alcohol abuse [4]. Currently, lifestyle change, including proper diet plans and exercises, is the most basic therapy strategy for patients with NAFLD [5]. However, most patients cannot complete the designed plan, resulting in less than satisfactory treatment outcomes [5]. At present, NAFLD has no approved pharmacological treatments [6]. NAFLD will develop into steatohepatitis, cirrhosis, and even cancer if patients with NAFLD delay treatment [5,7]. Hence, investigating the potential drugs is important to prevent NAFLD.

Liver fibrosis, which is characterized by extracellular matrix deposits, results from advanced liver damage and is intimately linked to cirrhosis and liver cancer [8]. One-third of patients with NAFLD develop liver fibrosis in 4–5 years [9]. Liver fibrosis deterioration is an important NAFLD outcome indicator [10,11]. Thus, liver fibrosis amelioration is an important indicator of the efficacy of drugs for NAFLD therapy. Hence, research into molecular mechanisms and the search for targets and drugs to alleviate liver fibrosis is important for treating NAFLD.

Hepatic stellate cells (HSCs) are the main matrix-secreting cells and exert critical function in liver fibrosis development [12,13]. HSCs are activated after liver damage, making the cells acquire proliferative and contractile characteristics, thereby expressing alpha-smooth muscle actin (α-SMA) and extracellular matrix [14,15]. Therefore, activity regulation of HSCs is essential for alleviating liver fibrosis. For example, Arroyo *et al.* [15] revealed that GATA4 repressed liver fibrosis via HSC deactivation. Zong *et al.* [16] found that nicotinamide mononucleotide restrained HSC activity and alleviated fibrosis.

In this study, we constructed the gerbil NAFLD-associated fibrosis model, screened differentially expressed genes in this model, and investigated the role of a significantly upregulated gene in NAFLD-associated fibrosis and its possible mechanism.

2. Materials and Methods

2.1 Animals

The Experimental Animal Center of Zhejiang Academy of Medical Sciences (Hangzhou, China) offered 24 male 90-day-old Mongolian gerbils (*Merionesunguiculatus*). The animal experiments were approved by the local Ethics Committee of the Zhejiang Academy of Medical Sciences (approved number 2019-056) and were conducted the recommendations in the Guide for the Care and Use of Laboratory Animals of the National Institutes of Health.

2.2 High-Fat and High-Cholesterol Diet (HFD) to Induce NAFLD and Fibrosis

Gerbils were allocated into the normal (n = 6) and model groups (n = 18). The normal group received a normal diet for 16 weeks. The model group received the HFD for 8, 12, and 16 weeks (n = 6 per group). The HFD recipes for inducing NAFLD and fibrosis models are referred to in our previously reported paper [17]. The HFD consists of 80.3% of ordinary feed, 10% of egg yolk powder, 7% lard oil, 2.5% cholesterol, and 0.2% cholate.

2.3 Experimental Design

The model group was sacrificed for dynamic mechanical studies at 8, 12, and 16 weeks. The normal group was spared at week 16. Abdominal aorta blood was harvested [18], and serums were prepared using centrifugation (3500 $\times g$, 10 min) to measure the alanine transaminase (ALT), aspartate transaminase (AST), and hydroxyproline (Hyp) levels. The central portion of the largest liver lobe was removed to make homogenate for Zinc Finger and BTB Domain Containing 14 (Zbtb14) expression determination. Another part of the liver sample was used for histopathological evaluation.

2.4 Histopathology

Hematoxylin and eosin, Masson's trichrome, and Sirius red staining were performed on liver tissues for the histopathological study using the microscope (Leica DM2500, Wetzlar, Germany). A single-blinded pathologist evaluated liver damage, inflammation, and fibrosis, following the scoring criteria described in a previous study [19]. Ten random areas were obtained from each liver slice.

2.5 Biochemical Analysis

The serum contents of ALT (Cat No. BC1555), AST (Cat No. BC1565; all from Beijing Solarbio Science & Technology Co., Ltd, Beijing, China), and Hyp (Cat No. A030-1; Jiancheng Biotech. Sci. Inc., Nanjing, China) were determined by Commercial kits following the provider's instructions.

2.6 High-Throughput mRNA Sequencing and Unigene Annotation

High-throughput mRNA sequencing was accomplished in LC-BIO Technologies (Hangzhou, China) Co., Ltd. Trizol reagent (Invitrogen, Carlsbad, CA, USA) was used to isolate RNA samples. A 2100 Bioanalyzer was used for quantification, and RNA 6000 Nano LabChip Kit (Agilent, Santa Clara, CA, USA) was used for purification. Afterward, short fragments were prepared from the purified mRNA. Then, the mRNA-Seq sample preparation kit (Illumina, San Diego, CA, USA) was applied to construct the cDNA library. Sequencing was conducted on the Hiseq4000 platform by the 150PE strategy. The cleaned reads were assembled *de novo* by Trinity version 2.4.0 (Broad Institute, Cambridge, MA, USA). The transcripts were clustered, and the unigenes were searched against the Gene Ontology (GO) database.

2.7 Differentially Expressed Genes (DEGs) Identification

The DEGs between the normal and model groups at 16 weeks were screened using Limma (3.32.5) with the criteria, $p < 0.05$ and $|\log FC| > 1$. Hierarchical clustering was completed on the DEGs from the three gene sets obtained by pairwise stage comparisons using Pheatmap package in R version 4.0.3 (POSIT Software, Boston, MA, USA), and the heatmap was established. Enriched GO terms were determined by Metascape version 3.32.5 (FDR (False Discovery Rate) <0.05) according to the analysis of mouse homologous sequences.

2.8 Cell Culture

Primary HSCs were harvested from gerbil livers treated with or without the HFD for 16 weeks following previously reported protocols [20]. The livers were digested with 1 mg/mL of pronase, 0.4 mg/mL of collagenase IV, and 0.2 mg/mL of DNase I at 37 °C for 30 min. Then, the tissues were made into pieces and digested again for 15 min. Subsequently, Dulbecco's Modified Eagle Medium (DMEM) with 10% fetal bovine serum (FBS) (HyClone, Logan, UT, USA) was used to finish the digestion. The digestive tissues were filtered, and the filtrate was centrifuged and removed from the supernatant. Afterward, cells were resuspended in DMEM, and 39.5% of percoll solution (Solarbio, Beijing, China) was mixed into the cells to separate HSCs. The HSCs were cultured using DMEM plus 10% FBS with or without 10 µM of XAV-939 (Selleck Chemicals, Shanghai, China), which is a Wnt/β-catenin pathway inhibitor. The HSCs were confirmed by detecting the α-SMA expression by quantitative reverse transcription polymerase chain reaction (RT-qPCR) and western blotting. This study used the first passage of HSCs.

2.9 Cell Transfection

Small interfering RNAs (siRNAs) were used for gene silencing. Two Zbtb14 siRNAs (siZbtb14-1: 5′-GCGACAUGAAGUUCGAGUAUC-3′ and siZbtb14-

2: 5′-GGACGACGACGUGGAAGAAAU-3′) were constructed by Genepharm Technologies (Shanghai, China). The coding sequence of Zbtb14 was inserted into pcDNA3.1(+) (Addgene) to synthesize the Zbtb14 overexpression plasmid. The siRNA or overexpression vector was transfected into primary HSCs by applying Lipofectamine 2000 (Invitrogen). The scramble siRNA (siNC) or blank pcDNA3.1(+) vector was designated for the negative control.

2.10 Cell Viability Assay

Primary HSCs were maintained in a 96-well plate and treated with 10 µL of Cell Counting Kit-8 (CP002; Signalway Antibody, Greenbelt, MA, USA) for 60 min. OD450 nm was observed.

2.11 Enzyme-Linked Immunosorbent Assay

The contents of types I (Cat No. CSB E08083m) and III collagen (Cat No. CSB E07925m) in cell supernatant were tested by Commercial kits (CUSABIO, Houston, TX, USA) following the stated protocols by the supplier.

2.12 RT-qPCR

A total of 5 µg of RNA samples were harvested by TRIzol and used for producing cDNAs utilizing the Hifair® II 1st Strand cDNA Synthesis SuperMix for qPCR (gDNA digester plus) (Cat No. 11123ES60, Yesen, Shanghai, China). The SYBR®Green reagent (Thermo Fisher Scientific, Waltham, MA, USA) was applied to ABI PRISM 7300 RT-PCR system (Applied Biosystems, Hammonton, NJ, USA) to complete the qPCR assay. The relative expression was obtained using the $2^{-\Delta\Delta Ct}$ method by designating GAPDH as the control gene. Primers used were (5′-3′): Zbtb14: AAGTCTCCCACGACCACCC (F), TCTTTCACTTCGCTCATCCC (R); α-SMA: CAGGGAGTGATGGTGGGG (F), TTAGCAGGGTCGGGTGC (R); Gapdh: GTCGGAGTGAACGGATTTGG (F), TTCTCAGCCTTGACTGTGCC (R); ZBTB14: CAAGTCGCCCACCACAAC (F), CGCCTGGCAGGCAATC (R); GAPDH: TCCCATCACCATCTTCCAGG (F), GATGACCCTTTTGGCTCCC (R).

2.13 Western Blotting

RIPA reagent (Sigma-Aldrich, St. Louis, MO, USA) was used to collect protein samples, and the bicinchoninic acid assay method was used to determine the concentration measurement. Then, 25 µg of proteins were run on the SDS-PAGE, blotted to PVDF membranes, and probed to primary and secondary antibodies. Antibodies included anti-ZBTB14 (Santa Cruz, Santa Cruz, CA, USA; sc-514298), anti-α-SMA (Cell Signaling Technology, Danvers, MA, USA; 19245T), anti-MMP2 (Abcam, Waltham, MA, USA; ab92536), anti-Cyclin D1 (Abcam; ab16663), anti-β-catenin (Abcam; ab32572), anti-H3 (Abcam; ab1791), and anti-GAPDH (Proteintech, Rosemont, IL, USA; 60004-1-Ig). Bands were visualized with ECL (Biovision Inc, Mountain View, CA, USA).

2.14 Clinical Samples

Liver tissue samples were obtained from 36 patients with liver fibrosis (Mild, n = 18, 44.4% male; Severe, n = 18, 44.4% male) who received liver biopsies from Sir Run Run Shaw Hospital, Affiliated with School of Medicine, Zhejiang University. Healthy normal liver tissues were obtained from 12 volunteers (age, 38.5 $\pm$ 10.4 years; 41.67% male). The study was performed following the Declaration of Helsinki and was approved by the Ethics Committee of the Sir Run Run Shaw Hospital, Affiliated with School of Medicine, Zhejiang University (approved number 2023-0062). All participants signed informed consent.

2.15 Statistical Analysis

Data are described as mean $\pm$ standard deviation or standard error, and analysis was completed by GraphPad Prism 8.4.2 (GraphPad Software, Inc., San Diego, CA, USA). The Mann-Whitney test was adopted to check the differences between the two groups. Data from multiple groups were compared via a one-way analysis of variance. All assays were conducted three times. p-values of <0.05 was considered statistically significant.

3. Results

3.1 Screening for DEGs in Gerbil NAFLD-Associated Fibrosis Model

The gerbil model was constructed by giving an HFD to investigate the mechanism of NAFLD-associated fibrosis development. Histological staining results indicated no discernible histological alterations in the normal gerbils, which were reflected by intact sinusoidal spaces, distinct nuclei, and central veins (Fig. 1A). However, the gerbils in the model group exhibited ballooning, denaturation, hepatocyte necrosis, and obvious fibrosis (Fig. 1A). Additionally, the model group presented elevated serum ALT, AST, and Hyp levels compared to the normal group ($p < 0.001$, Fig. 1B–D).

High-throughput mRNA sequencing was performed to screen DEGs to better study the pathogenesis of NAFLD-associated fibrosis. Principal Component Analysis (PCA) analysis of genes profiles of liver tissues isolated from gerbils revealed that the model samples appeared separated from normal samples (Fig. 1E), indicating the strongly differentiated expression profile of the model group from the normal group. The DEGs between the two groups were analyzed, and the heatmap of the DEGs was presented in Fig. 1F. The top 10 upregulated and downregulated genes in the model group were described in Tables 1,2, respectively. Additionally, GO annotations analysis of the DEGs was conducted in the aspects of molecular function, biological process, and cellular component. The molecu-

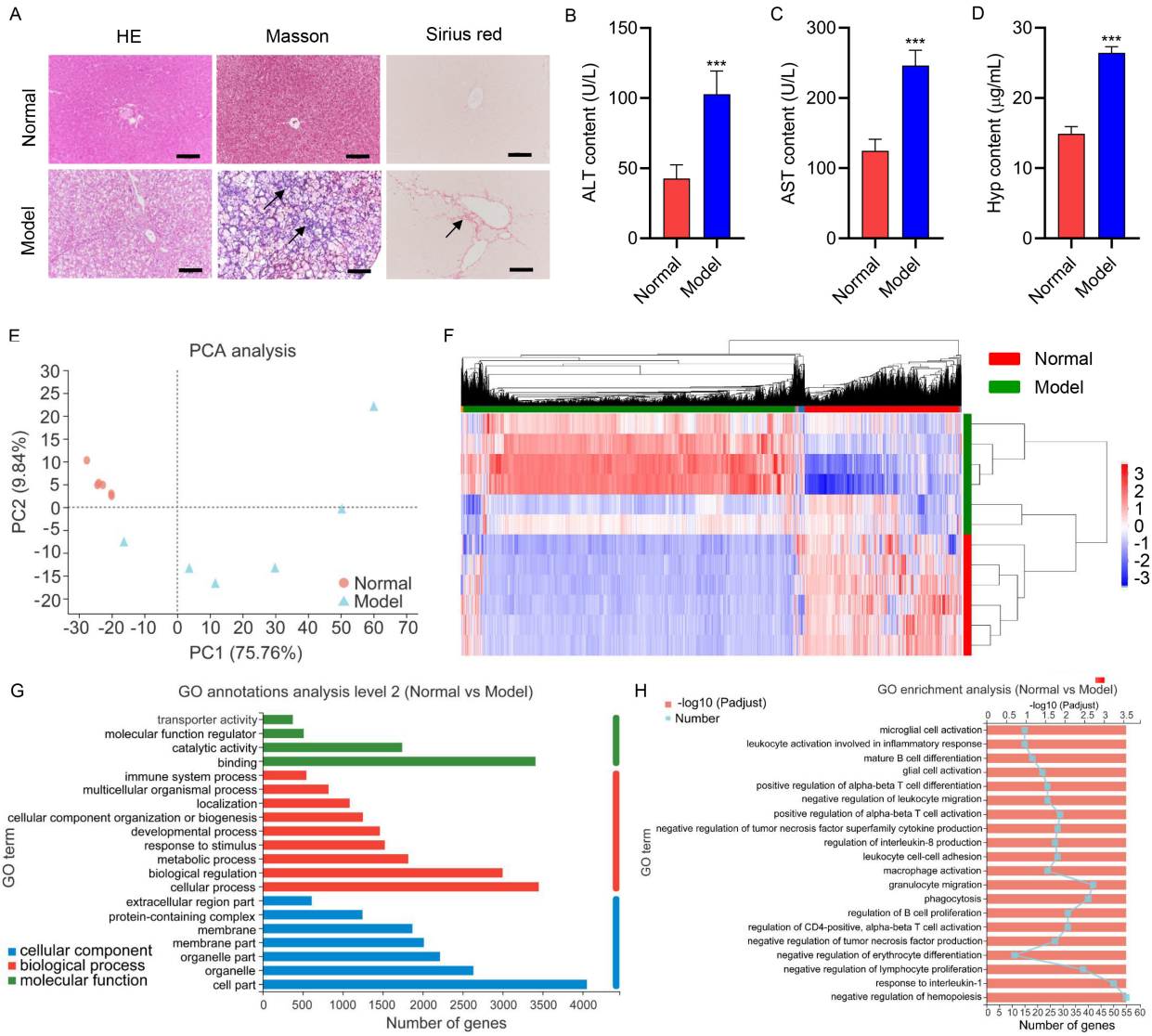

Fig. 1. Hepatic injury of gerbils during the high-fat and high-cholesterol diet. Gerbils were treated with the HFD for 16 weeks (Model; n = 6). Untreated gerbils were used as the normal control group (Normal; n = 6). (A) Representative HE, Masson, and Sirius red stained section of liver tissues (scale bar, 100 μm). Arrows indicated the fibrotic lesion localization. Serum (B) ALT, (C) AST, and (D) Hyp concentrations. (E) PCA analysis of genes profiles of liver tissues isolated from gerbils. (F) Heatmap of the differentially expressed genes. (G) GO annotations analyze the differentially expressed genes in molecular function, cellular components, and biological processes. (H) GO enrichment analysis of the differentially expressed genes. ***$p < 0.001$ vs. normal. ALT, alanine transaminase; AST, aspartate transaminase; Hyp, hydroxyproline; PC2, principal component 2; PCA, principal component analysis; PC1, principal component 1; GO, Gene Ontology; HE, Hematoxylin and eosin.

lar function includes "binding", "catalytic activity", and "molecular function regulator" as key functions involved by DEGs (Fig. 1G). DEGs were closely related to the "cellular process", "biological regulation", and "metabolic process" in the biological processes (Fig. 1G). DEGs were principally associated with the "cell part", "organelle", and "organelle part" in the cellular components (Fig. 1G). Furthermore, GO enrichment results demonstrated that DEGs were chiefly enriched in "negative regulation of hemopoiesis", "response to interleukin-1", and "granulocyte migration" (Fig. 1H).

3.2 Zbtb14 was Upregulated in the Gerbil NAFLD-Associated Fibrosis Model and Patients with Liver Fibrosis

Among DEGs, *Zbtb14* was one of the top 10 upregulated genes in the gerbil NAFLD-associated fibrosis model. However, the role of *Zbtb14* in NAFLD-associated fibrosis remained elusive. The Zbtb14 expression was first verified in gerbils after being treated with the HFD for 8, 12, and 16 weeks to explore its function in NAFLD-associated fibrosis. Results indicated increased Zbtb14 in the liver of gerbils in the 8-, 12-, and 16-week groups versus the

Table 1. Top ten upregulated genes in a gerbil model of NAFLD associated fibrosis.

Gene name	Log_2 (Model/Normal)	*p* value	*p* adjust	Normal	Model
Mast3	1.935	1.38×10^{-34}	1.25×10^{-31}	0.752	6.650
Bmf	2.822	4.32×10^{-31}	2.61×10^{-28}	0.587	9.392
Znf148	1.218	3.39×10^{-25}	1.18×10^{-22}	0.733	4.402
Usp33	1.072	4.28×10^{-25}	1.46×10^{-22}	1.753	8.338
Mmp12	5.760	2.19×10^{-22}	5.74×10^{-20}	1.887	261.7
Tdp2	1.440	5.62×10^{-21}	1.27×10^{-18}	1.333	8.300
Colec12	6.666	2.16×10^{-20}	4.65×10^{-18}	0.345	89.96
Zbtb14	1.555	4.83×10^{-20}	9.93×10^{-18}	1.708	11.83
Fbxo11	1.072	8.48×10^{-20}	1.67×10^{-17}	2.462	11.75
Ppargc1b	3.630	1.14×10^{-19}	2.22×10^{-17}	0.058	1.720

NAFLD, non-alcoholic fatty liver disease.

Table 2. Top ten downregulated genes in a gerbil model of NAFLD associated fibrosis.

Gene name	Log_2 (Model/Normal)	*p* value	*p* adjust	Normal	Model
Socs3	–4.33249	6.33×10^{-233}	1.15×10^{-228}	100.7	10.84
Csrnp1	–3.57326	1.76×10^{-127}	1.59×10^{-123}	16.58	3.022
Rasd1	–7.8831	9.56×10^{-98}	5.77×10^{-94}	39.35	0.368
Btg2	–4.61946	2.03×10^{-95}	9.18×10^{-92}	94.39	8.588
LOC110557684	–3.12558	6.57×10^{-95}	2.38×10^{-91}	10.13	2.597
Irs2	–5.72892	3.83×10^{-58}	1.16×10^{-54}	66.78	2.782
Gadd45g	–4.07069	5.33×10^{-58}	1.38×10^{-54}	90.33	11.52
Midn	–1.99354	4.42×10^{-57}	1.00×10^{-53}	35.63	19.75
Spidr	–1.54349	1.60×10^{-53}	3.21×10^{-50}	6.655	5.083
Irf1	–2.92794	6.33×10^{-52}	1.15×10^{-48}	73.13	20.33

Table 3. Clinicopathological characteristics and follow-up data of patients with liver fibrosis.

Characteristics	*ZBTB14* mRNA expression		*p* value
	Low (n = 18)	High (n = 18)	
Gender			0.502
Male (n = 16)	7	9	
Female (n = 20)	11	9	
Age (years)			0.172
<48 (n = 14)	9	5	
≥48 (n = 22)	9	13	
Type 2 diabetes n (%)	10 (55.5%)	15 (83.3%)	0.070
Body mass index (kg/m^2)	30.9 ± 3.8	31.8 ± 3.4	0.420
Total cholesterol (mg/dL)	191.6 ± 20.2	186.4 ± 16.3	0.438
HDL cholesterol (mg/dL)	50.2 ± 11.4	47.5 ± 10.9	0.496
LDL cholesterol (mg/dL)	103.3 ± 31.1	111.8 ± 23.3	0.536
Triglycerides (mg/dL)	151.1 ± 53.6	166.1 ± 57.6	0.424
AST (U/L)	37.9 ± 15.2	56.0 ± 24.4	0.012
ALT (U/L)	49.5 ± 26.2	72.8 ± 27.0	0.014
HbA1c (%)	6.19 ± 0.66	6.63 ± 0.49	0.042

AST, aspartate aminotransferase; ALT, alanine aminotransferase; HDL, high density lipoprotein; LDL, low density lipoprotein; HbA1c, glycated hemoglobin. Differences between groups were determined by the Chi-square test or Mann-Whitney test.

normal group ($p < 0.001$, Fig. 2A,B). Moreover, primary HSCs were obtained from gerbils treated with or without the HFD for 16 weeks. The α-SMA expression in HSCs was determined. The α-SMA elevation in HSCs of the gerbil model ($p < 0.001$, Fig. 2C,D) indicated HSC activation. Moreover, Zbtb14 increased in the activated HSCs of the model ($p < 0.001$, Fig. 2C,D). Furthermore, the *ZBTB14* level was elevated in liver tissues of patients with mild and severe liver fibrosis ($p < 0.001$, Fig. 2E). Table 3 provides a detailed clinical and biochemical profile of patients with liver fibrosis. Patients with higher *ZBTB14* mRNA expression demonstrated higher AST, ALT, and hemoglobin A1c levels ($p < 0.05$). Interestingly, elevated *ZBTB14* was observed in severe patients versus mild patients ($p < 0.001$, Fig. 2E). Therefore, Zbtb14 was elevated in the gerbil NAFLD-associated fibrosis model and patients with liver fibrosis.

3.3 Zbtb14 Knockdown Suppressed Primary HSCs Activation

The role of aberrant expressed Zbtb14 in HSC activation was identified to further study the function of Zbtb14 on NAFLD-associated fibrosis. HSCs obtained from gerbils treated with the HFD for 16 weeks were transfected with the siRNA against *Zbtb14*. Results revealed that the silenced *Zbtb14* notably inhibited the cell viability of HSCs ($p < 0.001$, Fig. 3A). Additionally, silenced *Zbtb14* suppressed the Hyp content and collagen I and III concentrations in HSCs ($p < 0.001$, Fig. 3B,C). Expectedly, the

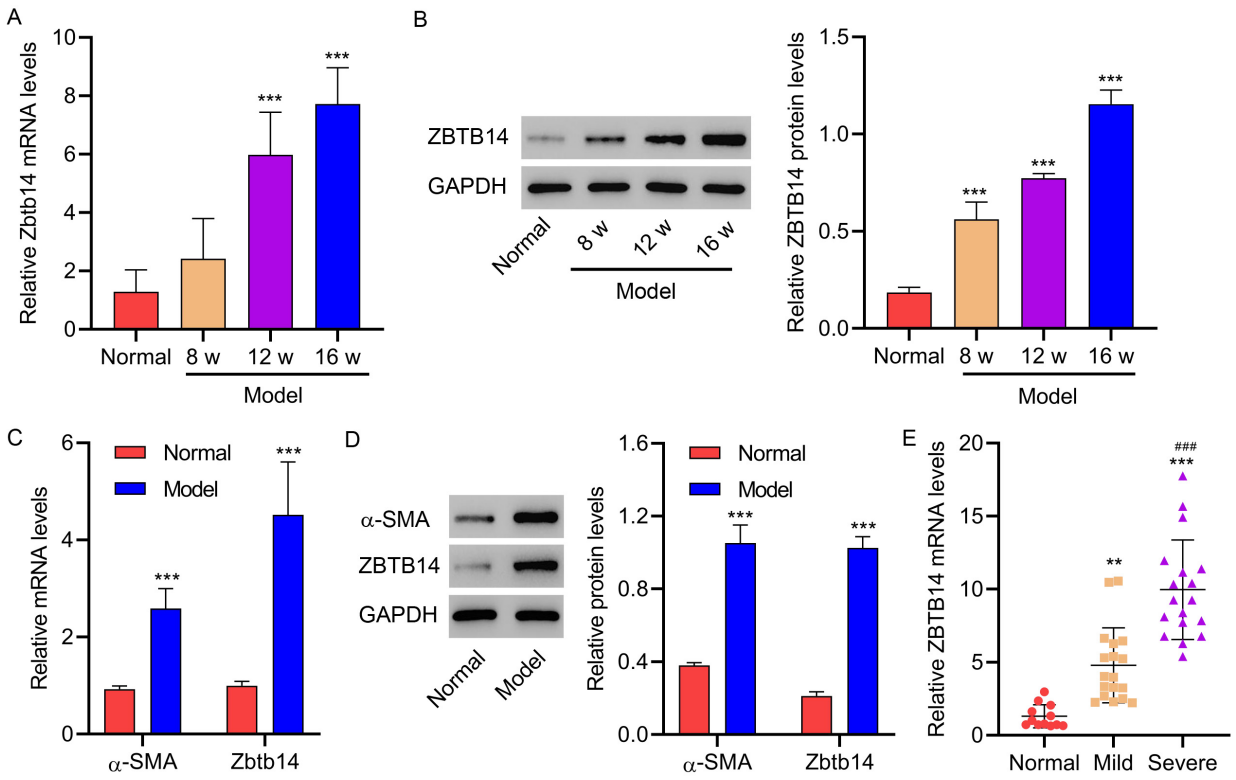

Fig. 2. Zbtb14 expression in gerbils and patients with fibrosis. Gerbils were treated with the HFD for 8, 12, or 16 weeks (Model; n = 6 per group). Untreated gerbils were used as the normal control group (Normal; n = 6). (A,B) Zbtb14 expression in liver tissues isolated from gerbils. (C,D) α-SMA and Zbtb14 expression in primary HSCs isolated from gerbils treated with or without a high-fat and high-cholesterol diet for 16 weeks (n = 3 per group). (E) *ZBTB14* expression in liver tissues was collected from patients with liver fibrosis (Mild, n = 18; Severe, n = 18) or healthy control (n = 12). $^{**}p < 0.01$, $^{***}p < 0.001$ vs. normal; $^{\#\#\#}p < 0.001$ vs. mild.

Zbtb14 knockdown remarkably restrained the protein levels of Zbtb14, α-SMA, MMP2, Cyclin D1, and β-catenin in HSCs ($p < 0.001$, Fig. 3D,E). Therefore, *Zbtb14* knockdown suppressed primary hepatic stellate cell activation.

3.4 Zbtb14 Overexpression Promoted Primary HSC Activation via the β-Catenin Pathway

To better determine the function of Zbtb14 on HSC activation and the underlying mechanism, the HSCs were transfected with *Zbtb14* overexpression vector with or without XAV939 (inhibitor of β-catenin signaling) treatment. Overexpressed *Zbtb14* notably enhanced the viability of HSCs, which was abolished by XAV939 ($p < 0.001$, Fig. 4A). Additionally, the promotion effects of overexpressed *Zbtb14* on the Hyp content and collagen I and III concentrations were abrogated by XAV939 ($p < 0.001$, Fig. 4B,C). Moreover, the *Zbtb14* overexpression vector remarkably increased the Zbtb14 level ($p < 0.001$), while XAV939 treatment did not affect Zbtb14 expression (Fig. 4D,E). Furthermore, *Zbtb14* overexpression increased the α-SMA, MMP2, Cyclin D1, and β-catenin levels, which was reversed by XAV939 ($p < 0.001$, Fig. 4D,E). Hence, *Zbtb14* overexpression promoted primary HSC activation via the β-catenin pathway.

4. Discussion

NAFLD is a popular chronic liver disorder with high morbidity worldwide [1–3]. Currently, no drug is approved for NAFLD treatment [6]. Liver fibrosis is considered an important predictor of the efficacy of drugs for NAFLD therapy [10,11]. Hence, the possible mechanisms of liver fibrosis should be elucidated and targets to prevent liver fibrosis and NAFLD should be determined.

The gerbil model of NAFLD with fibrosis was first established to study the mechanism of NAFLD-associated liver fibrosis. In this model, denaturation and necrosis were observed in liver tissues. Additionally, liver function was evaluated by determining serum ALT and AST levels. ALT is an abundant enzyme in hepatocytes [21]. The serum ALT level increased after hepatocytes were injured [21]. Therefore, ALT usually indicates hepatic inflammation and injury in NAFLD [21]. AST is another biochemical marker of liver injury, which is released into the bloodstream after liver injury [22]. This study revealed increased ALT and AST levels in the NAFLD-associated fibrosis model, indicating that liver injury was induced in the gerbil.

Furthermore, obvious fibrosis was presented in the liver tissues of the gerbil model. The Hyp level is determined to confirm the finding. Hyp determination was

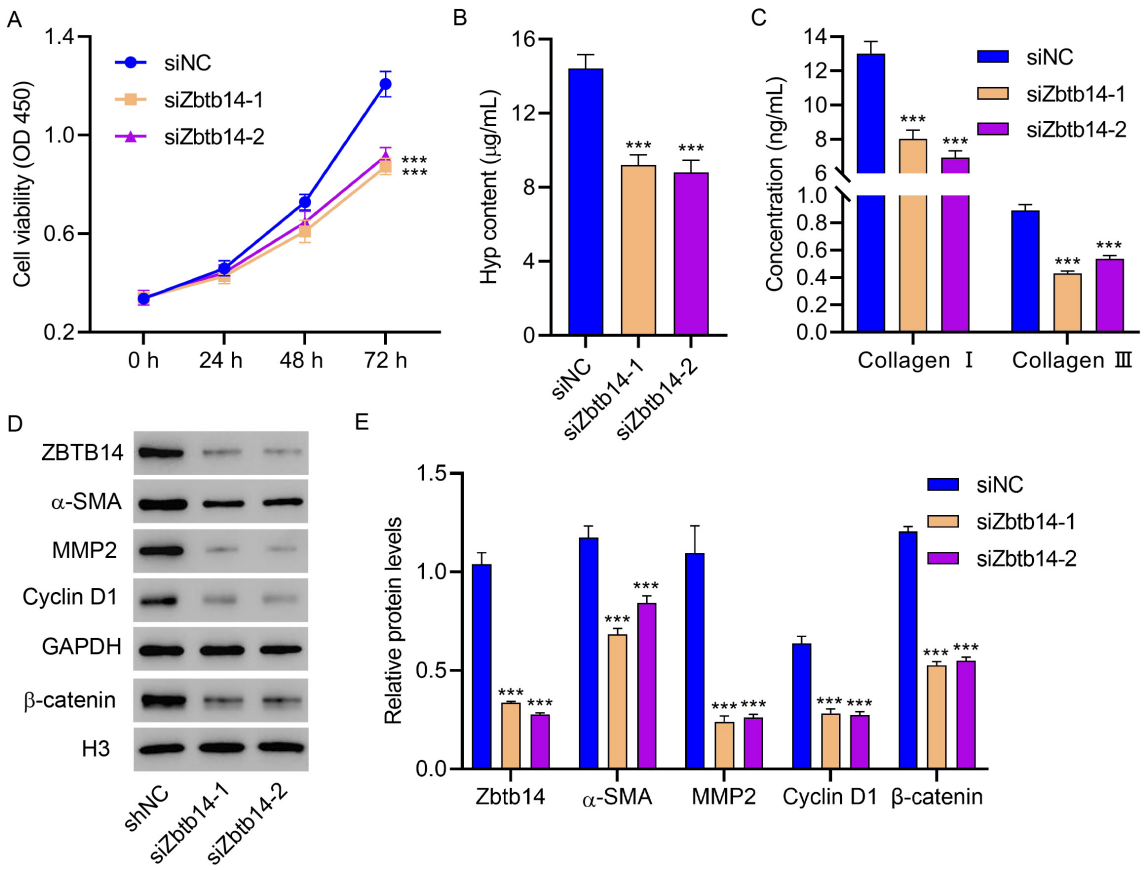

Fig. 3. *Zbtb14* knockdown inhibits primary HSC activation. Primary HSCs isolated from gerbils treated with the HFD for 16 weeks were transfected with *Zbtb14* siRNA, and the (A) cell viability, (B) Hyp, (C) type I collagen, and type III collagen levels, and (D,E) Zbtb14, α-SMA, MMP2, Cyclin D1, and β-catenin expression were determined. ***$p < 0.001$ vs. siNC.

a common strategy for assessing tissue fibrosis and collagen deposition [23,24]. Results revealed elevated Hyp levels in the gerbil NAFLD model, consistent with the previous study [25]. These findings demonstrated a successful NAFLD-asLociated fibrosis model construction.

DEGs in the NAFLD-associated fibrosis model were screened using high-throughput mRNA sequencing to explore the pathogenesis of the NAFLD-associated fibrosis model. GO enrichment results proved that DEGs were mainly gathered in "negative regulation of hemopoiesis", "response to interleukin-1", and "granulocyte migration". Shvarts *et al.* [26] revealed suppressed hemopoiesis in CCl(4)-induced hepatic fibrosis. Additionally, the production of the members of the interleukin-1 family exerted a critical function in NAFLD [27]. Furthermore, neutrophils, which are the most abundant type of granulocyte, were activated and migrated from the blood to the tissues in NAFLD [28]. The above evidence suggested that the biological processes mainly enriched by DEGs, including "negative regulation of hemopoiesis", "response to interleukin-1", and "granulocyte migration", were significant for NAFLD-associated fibrosis.

ZBTB14, also known as ZNF478 and ZFP161, is a zinc finger protein classified as the ZBTB family [29]. This study revealed Zbtb14 as one of the top 10 upregulated genes in the NAFLD-associated fibrosis model. Interestingly, Zbtb14 was demonstrated to modulate hemopoiesis [30]. Therefore, Zbtb14 was selected to further study its role in NAFLD-associated fibrosis. Western blot and RT-qPCR results, consistent with high-throughput mRNA sequencing, verified that Zbtb14 was enhanced in the NAFLD-associated fibrosis model and patients with liver fibrosis. Additionally, results revealed that Zbtb14 was elevated in activated HSCs. The function of Zbtb14 in HSCs activation was investigated by determining cell viability and activation markers because HSCs are vital in liver fibrosis development [12,13]. Results revealed that *Zbtb14* knockdown suppressed primary HSCs viability and the α-SMA, MMP2, Hyp, and collagen I and III levels. α-SMA is considered a reliable marker of HSC activation [31]. Activated HSCs could produce α-SMA and collagen [14,15], as well as collagen-induced MMP2 activation and expression [32]. Hence, the findings indicated that *Zbtb14* knockdown suppressed primary HSC activation. This study first reported elevated Zbtb14 in NAFLD-associated fibrosis and regulated HSC activation.

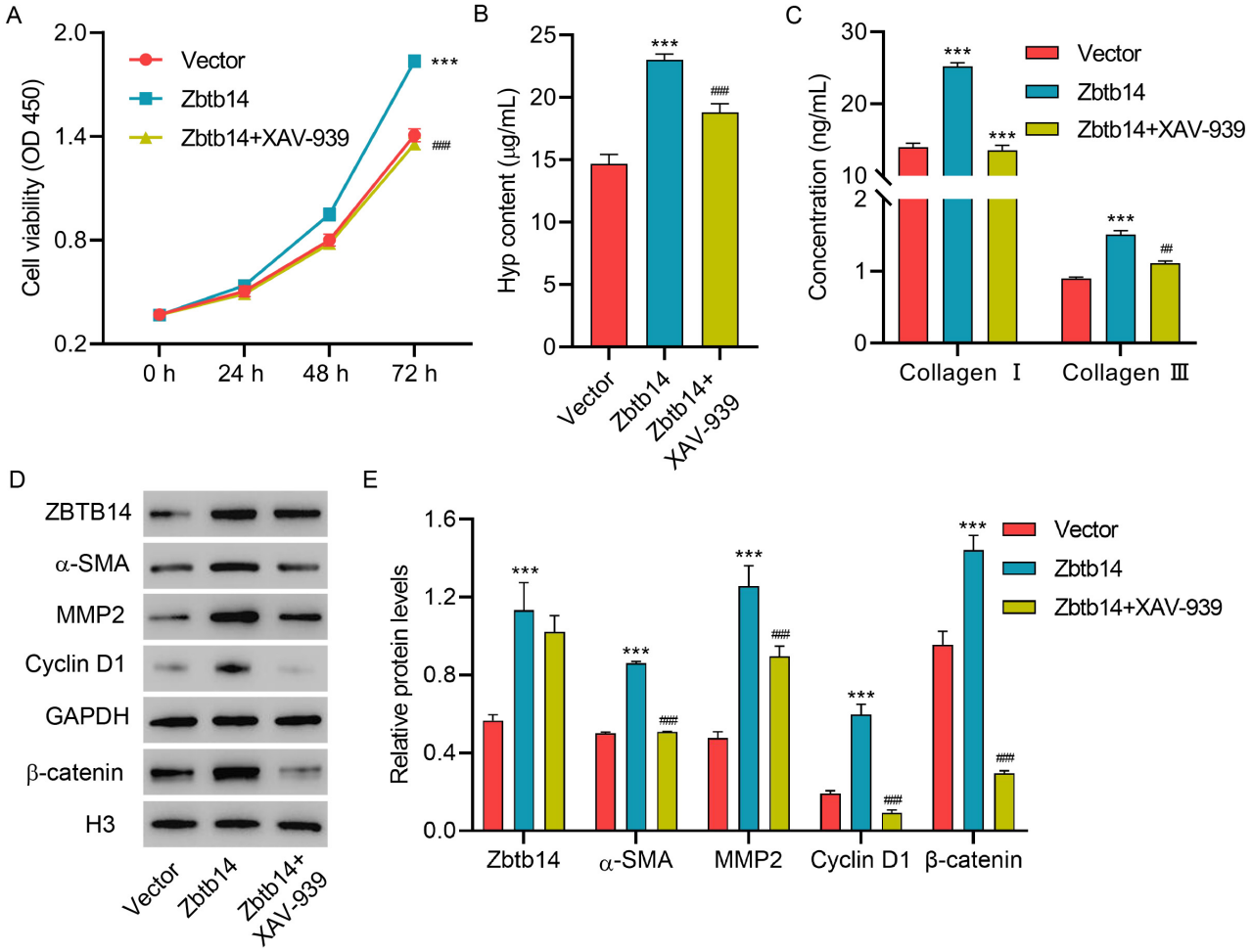

Fig. 4. *Zbtb14* overexpression promotes primary HSC activation via the β-catenin pathway. Primary HSCs isolated from untreated gerbils were transfected with *Zbtb14* overexpression vector with or without XAV939 treatment, and the (A) cell viability, (B) Hyp, (C) type I collagen, and type III collagen levels and (D,E) Zbtb14, α-SMA, MMP2, Cyclin D1, and β-catenin expressions were determined. $^{***}p < 0.001$ vs. vector; $^{\#\#}p < 0.01$, $^{\#\#\#}p < 0.001$ vs. Zbtb14.

The β-catenin pathway is critical in tissue homeostasis, including the liver [33]. Ge *et al.* [33] revealed upregulated β-catenin in hepatic fibrosis and suppressed HSCs activation by β-catenin signaling inhibition. This study revealed that silenced *Zbtb14* suppressed the β-catenin and Cyclin D1 levels. Therefore, we inferred that the β-catenin pathway might mediate Zbtb14 regulation on HSC activation. Expectedly, results revealed the abolished regulation effects of Zbtb14 on the α-SMA, MMP2, Hyp, and collagen I and III by the β-catenin pathway inhibitor. Hence, we concluded that Zbtb14 regulated primary HSC activation via the β-catenin pathway. In particular, Zbtb14 modulated NAFLD-associated fibrosis in gerbils via the β-catenin pathway.

The additional diet cholesterol may cause some metabolism differences, which is the remaining limitation of the gerbil model. Further studies are required to address whether alterations in diet composition can lead to a refined model, which can completely reproduce the human disease mechanism. Additionally, a large portion of expressed genes generally show sex-specific differences in the liver, and diet effects could conceivably be confounded by sex effects. Only male gerbils were used in the present study. Therefore, further examination of NAFLD-associated fibrosis in female gerbils would be meaningful and more reliable.

5. Conclusions

In conclusion, this study identified the DEGs in NAFLD-associated fibrosis and reported Zbtb14 modulated NAFLD-associated fibrosis in male gerbils via the β-catenin pathway for the first time. Zbtb14 serves as the probable target for NAFLD therapy.

Availability of Data and Materials

The datasets used and/or analyzed during the current study are available from the corresponding author on reasonable request.

Author Contributions

GC and XC designed the research study. XW, YZ, and HH performed the research. GC, XW, and XC provided help and advice on conception, acquisition of data, and supervision. YZ, HH, and XC analyzed the data. GC wrote the manuscript. All authors contributed to editorial changes in the manuscript. All authors read and approved the final manuscript. All authors have participated sufficiently in the work and agreed to be accountable for all aspects of the work.

Ethics Approval and Consent to Participate

The study was performed in accordance with the Declaration of Helsinki and was approved by the Ethics Committee of the Sir Run Run Shaw Hospital, Affiliated with the School of Medicine, Zhejiang University (approved number 2023-0062). The animal experiments were approved by the local Ethics Committee of the Zhejiang Academy of Medical Sciences (approved number 2019-056) and were carried out in strict accordance with the recommendations in the Guide for the Care and Use of Laboratory Animals of the National Institutes of Health. All participants provided written informed consent to participate in the study after the procedures had been completely explained.

Acknowledgment

Not applicable.

Funding

This research was funded by the National Natural Science Foundation of China (31970511) and Zhejiang province commonweal projects (LGD20C040003).

Conflict of Interest

The authors declare no conflict of interest.

References

[1] Friedman SL, Neuschwander-Tetri BA, Rinella M, Sanyal AJ. Mechanisms of NAFLD development and therapeutic strategies. Nature Medicine. 2018; 24: 908–922.

[2] Berardo C, Di Pasqua LG, Cagna M, Richelmi P, Vairetti M, Ferrigno A. Nonalcoholic Fatty Liver Disease and Non-Alcoholic Steatohepatitis: Current Issues and Future Perspectives in Preclinical and Clinical Research. International Journal of Molecular Sciences. 2020; 21: 9646.

[3] Zeng T, Chen G, Qiao X, Chen H, Sun L, Ma Q, *et al*. NUSAP1 Could be a Potential Target for Preventing NAFLD Progression to Liver Cancer. Frontiers in Pharmacology. 2022; 13: 823140.

[4] Chen K, Ma J, Jia X, Ai W, Ma Z, Pan Q. Advancing the understanding of NAFLD to hepatocellular carcinoma development: From experimental models to humans. Biochimica et Biophysica Acta. Reviews on Cancer. 2019; 1871: 117–125.

[5] Hu M, Zhang L, Ruan Z, Han P, Yu Y. The Regulatory Effects of Citrus Peel Powder on Liver Metabolites and Gut Flora in Mice with Non-Alcoholic Fatty Liver Disease (NAFLD). Foods. 2021; 10: 3022.

[6] Rinella ME, Sanyal AJ. Management of NAFLD: a stage-based approach. Nature Reviews. Gastroenterology & Hepatology. 2016; 13: 196–205.

[7] Tilg H, Moschen AR, Roden M. NAFLD and diabetes mellitus. Nature Reviews. Gastroenterology & Hepatology. 2017; 14: 32–42.

[8] Vilar-Gomez E, Calzadilla-Bertot L, Wai-Sun Wong V, Castellanos M, Aller-de la Fuente R, Metwally M, *et al*. Fibrosis Severity as a Determinant of Cause-Specific Mortality in Patients With Advanced Nonalcoholic Fatty Liver Disease: A Multi-National Cohort Study. Gastroenterology. 2018; 155: 443–457.e17.

[9] Su Q, Kumar V, Sud N, Mahato RI. MicroRNAs in the pathogenesis and treatment of progressive liver injury in NAFLD and liver fibrosis. Advanced Drug Delivery Reviews. 2018; 129: 54–63.

[10] Ekstedt M, Hagström H, Nasr P, Fredrikson M, Stål P, Kechagias S, *et al*. Fibrosis stage is the strongest predictor for disease-specific mortality in NAFLD after up to 33 years of follow-up. Hepatology. 2015; 61: 1547–1554.

[11] Yu X, Chen C, Guo Y, Tong Y, Zhao Y, Wu L, *et al*. High NAFLD fibrosis score in non-alcoholic fatty liver disease as a predictor of carotid plaque development: a retrospective cohort study based on regular health check-up data in China. Annals of Medicine. 2021; 53: 1621–1631.

[12] Puche JE, Saiman Y, Friedman SL. Hepatic stellate cells and liver fibrosis. Comprehensive Physiology. 2013; 3: 1473–1492.

[13] Tacke F, Weiskirchen R. Non-alcoholic fatty liver disease (NAFLD)/non-alcoholic steatohepatitis (NASH)-related liver fibrosis: mechanisms, treatment and prevention. Annals of Translational Medicine. 2021; 9: 729.

[14] Bataller R, Brenner DA. Hepatic stellate cells as a target for the treatment of liver fibrosis. Seminars in Liver Disease. 2001; 21: 437–451.

[15] Arroyo N, Villamayor L, Díaz I, Carmona R, Ramos-Rodríguez M, Muñoz-Chápuli R, *et al*. GATA4 induces liver fibrosis regression by deactivating hepatic stellate cells. JCI Insight. 2021; 6: e150059.

[16] Zong Z, Liu J, Wang N, Yang C, Wang Q, Zhang W, *et al*. Nicotinamide mononucleotide inhibits hepatic stellate cell activation to prevent liver fibrosis via promoting PGE_2 degradation. Free Radical Biology & Medicine. 2021; 162: 571–581.

[17] Li W, Guan Z, Brisset JC, Shi Q, Lou Q, Ma Y, *et al*. A non-alcoholic fatty liver disease cirrhosis model in gerbil: the dynamic relationship between hepatic lipid metabolism and cirrhosis. International Journal of Clinical and Experimental Pathology. 2018; 11: 146–157.

[18] Panchal SK, Poudyal H, Arumugam TV, Brown L. Rutin attenuates metabolic changes, nonalcoholic steatohepatitis, and cardiovascular remodeling in high-carbohydrate, high-fat diet-fed rats. The Journal of Nutrition. 2011; 141: 1062–1069.

[19] Kleiner DE, Brunt EM, Van Natta M, Behling C, Contos MJ, Cummings OW, *et al*. Design and validation of a histological scoring system for nonalcoholic fatty liver disease. Hepatology. 2005; 41: 1313–1321.

[20] Zhang H, Ju B, Nie Y, Song B, Xu Y, Gao P. Adenovirus mediated knockdown of activin A receptor type 2A attenuates immune induced hepatic fibrosis in mice and inhibits interleukin 17 induced activation of primary hepatic stellate cells. International Journal of Molecular Medicine. 2018; 42: 279–289.

[21] Ma X, Liu S, Zhang J, Dong M, Wang Y, Wang M, *et al*. Proportion of NAFLD patients with normal ALT value in overall NAFLD patients: a systematic review and meta-analysis. BMC Gastroenterology. 2020; 20: 10.

[22] Tian F, Chi F, Wang G, Liu X, Zhang Q, Chen Y, *et al*. Lactobacillus rhamnosus CCFM1107 treatment ameliorates alcohol-induced liver injury in a mouse model of chronic alcohol feeding. Journal of Microbiology. 2015; 53: 856–863.

[23] Kliment CR, Englert JM, Crum LP, Oury TD. A novel method for accurate collagen and biochemical assessment of pulmonary tissue utilizing one animal. International Journal of Clinical and Experimental Pathology. 2011; 4: 349–355.
[24] Woessner JF, Jr. The determination of hydroxyproline in tissue and protein samples containing small proportions of this imino acid. Archives of Biochemistry and Biophysics. 1961; 93: 440–447.
[25] Pellicano AJ, Spahn K, Zhou P, Goldberg ID, Narayan P. Collagen Characterization in a Model of Nonalcoholic Steatohepatitis with Fibrosis; A Call for Development of Targeted Therapeutics. Molecules. 2021; 26: 3316.
[26] Shvarts YS, Zubakhin AA, Dushkin MI. Suppression of hemopoiesis during CCl(4)-induced hepatic fibrosis: role of systemic endotoxemia. Bulletin of Experimental Biology and Medicine. 2000; 130: 759–762.
[27] Mirea AM, Tack CJ, Chavakis T, Joosten LAB, Toonen EJM. IL-1 Family Cytokine Pathways Underlying NAFLD: Towards New Treatment Strategies. Trends in Molecular Medicine. 2018; 24: 458–471.
[28] Lauszus JS, Eriksen PL, Hansen MM, Eriksen LL, Shawcross DL, Vilstrup H, *et al*. Activation and Functional Priming of Blood Neutrophils in Non-Alcoholic Fatty Liver Disease Increases in Non-Alcoholic Steatohepatitis. Clinical and Experimental Gastroenterology. 2021; 14: 441–449.
[29] Kim W, Zhao F, Wu R, Qin S, Nowsheen S, Huang J, *et al*. ZFP161 regulates replication fork stability and maintenance of genomic stability by recruiting the ATR/ATRIP complex. Nature Communications. 2019; 10: 5304.
[30] Deng Y, Wang H, Liu X, Yuan H, Xu J, de Thé H, *et al*. Zbtb14 regulates monocyte and macrophage development through inhibiting *pu.1* expression in zebrafish. ELife. 2022; 11: e80760.
[31] Shang L, Hosseini M, Liu X, Kisseleva T, Brenner DA. Human hepatic stellate cell isolation and characterization. Journal of Gastroenterology. 2018; 53: 6–17.
[32] Théret N, Lehti K, Musso O, Clément B. MMP2 activation by collagen I and concanavalin A in cultured human hepatic stellate cells. Hepatology. 1999; 30: 462–468.
[33] Ge WS, Wang YJ, Wu JX, Fan JG, Chen YW, Zhu L. β-catenin is overexpressed in hepatic fibrosis and blockage of Wnt/β-catenin signaling inhibits hepatic stellate cell activation. Molecular Medicine Reports. 2014; 9: 2145–2151.